Thin Solid Films 660 (2018) 601–605

Contents lists available at ScienceDirect

Thin Solid Films

journal homepage: www.elsevier.com/locate/tsf

# Residual stress control of Cu film deposited using a pulsed direct current magnetron sputtering

Tae Hyung Kim[a], Soo Jung Lee[a], Do Han Kim[a], Dong Woo Kim[a], Jeong Woon Bae[a], Kyong Nam Kim[c], Yong Mo Kim[d], Geun Young Yeom[a,b,*]

[a] Department of Materials Science and Engineering, Sungkyunkwan University, Suwon, Gyeonggi-Do 440-746, South Korea
[b] SKKU Advanced Institute of Nano Technology (SAINT), Sungkyunkwan University, Suwon, Gyeonggi-Do 440-746, South Korea
[c] Department of Advanced Materials, Daejeon University, 62 Daehak-ro, Dong-gu, Daejeon 300-716, Republic of Korea
[d] STC Division, Korea Instrument Co., Ltd., Hwaseong-si, Gyeonggi-Do 18487, Republic of Korea

ABSTRACT

Residual stress of 10 μm thick copper (Cu) film deposited using direct current (DC) magnetron sputtering system was analyzed for various pulsed DC power conditions. It is found that the increase of pulse frequency at a fixed duty ratio of 80% from continuous wave (CW) to 100 kHz while maintaining the time average power significantly decreased the residual stress of Cu film from 21.75 MPa to 1.8 MPa. The decrease of pulse duty ratio further decreased the residual stress by showing 0.7 MPa at 60% of duty ratio and 50 kHz pulse frequency. Therefore, compared to CW power, Cu film with ~1/30 lower residual stress could be deposited by using DC pulse power. The decrease of residual stress by pulsing and by decreasing the pulse duty ratio while keeping the same time average power was related to the denser film density and smaller grain size of deposited Cu film caused by increased instant sputter power during the pulsing.

## 1. Introduction

Heat dissipation of electronic devices is one of the most important reliability issues in manufacturing high performance electronics. Many researchers have investigated various methods in improving heat dissipation efficiency on various electric devices such as high power light emitting diodes and batteries because of the heat generated by high power consumption [1–3]. Also, many different methods have been proposed to remove the heat generated by electric devices [4,5]. However, due to the increased integration of the devices, more efficient cooling method is needed for better thermal management in using high power and highly integrated electronics, therefore, other techniques in improving the heat dissipation efficiency such as the application of carbon nanotube in polymer matrices [6–8], formation of a water-flow structure [9,10], formation of patterned fin or rod structure [11], etc. have been also studied.

As heat sink materials, copper (Cu) has been the most widely used material due to low cost and high heat dissipation efficiency. Generally, to deposit Cu at a high deposition rate on the substrate as the heat sink material, the electroplating method has been used. However, this method uses hazardous solutions, therefore, it can lead to environmental pollution during the waste water treatment. In addition, Cu deposited by the electroplating method tends to exhibit high residual stress, therefore, it may not be able to function as a heat sink material especially for a thick Cu film due to a high stress difference between Cu and substrate.

Magnetron sputter deposition has been used to deposit various thin and thick film materials including Cu films due to its high deposition rate, large area deposition, and ability to deposit most of materials. To improve the heat dissipation, a Cu film thicker than a few μm is required, and, when a thick Cu film is deposited by the magnetron sputtering, a failure of the devices such as bending of the substrate, detachment of Cu film from the substrate, etc. is observed due to the stress developed in the film. Recently, many researchers are investigating a pulsed power during the magnetron sputtering of various materials by varying pulse duty ratio or pulse frequency to control the plasma properties during the deposition on the substrates. By controlling the plasma properties through the pulsed magnetron sputtering, less target damage at the same power density and more uniform composition and higher step coverage of the deposited film have been obtained compared to the conventional direct current (DC) magnetron sputtering [12–18]. However, it is found that the control of residual stress of deposited metal film by using pulsed magnetron sputtering has not been investigated.

* Corresponding author at: Department of Materials Science and Engineering, Sungkyunkwan University, Suwon, Gyeonggi-Do 440-746, South Korea.
E-mail address: gyyeom@skku.edu (G.Y. Yeom).

https://doi.org/10.1016/j.tsf.2018.05.011
Received 19 December 2017; Received in revised form 4 May 2018; Accepted 5 May 2018
Available online 08 May 2018
0040-6090/ 

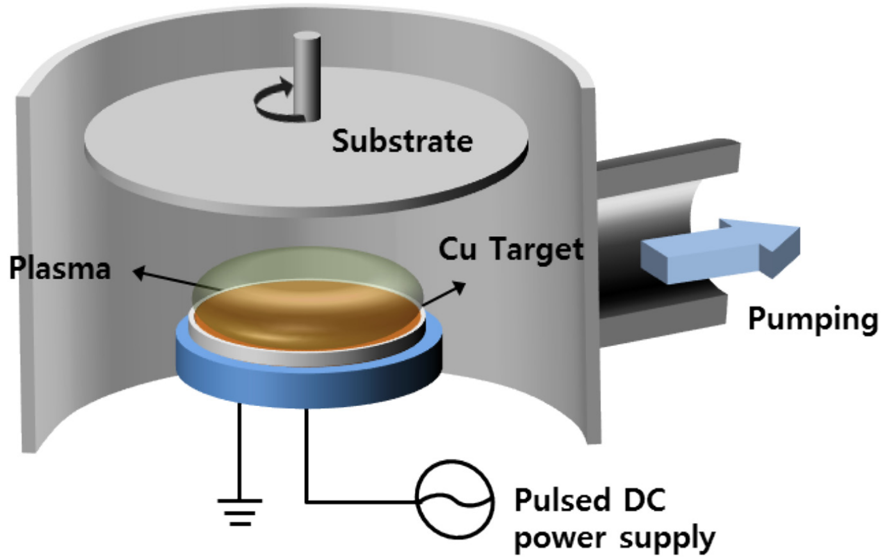


**Fig. 1.** Schematic diagram of the pulsed DC power magnetron sputter system used for depositing Cu film.

In this study, pulsed DC magnetron sputtering has been used to investigate the possible management of the residual stress in the deposited Cu film. The pulse frequency and pulse duty ratio of DC magnetron sputter power supply were varied while maintaining the time average power to control the residual stress of the Cu film. To study the mechanism related to the change of residual stress, the temporal change of voltage and current of the DC magnetron power, the change of ion energy on the substrate surface, and the microstructure of the deposited Cu film were investigated.

## 2. Experimental set-up

Fig. 1 shows the pulsed DC magnetron sputtering system used in the experiment. The size of the magnetron target was 3 in. diameter and the distance between the target and the substrate was ~10 cm. The base pressure was maintained $< 1.3 \times 10^{-3}$ Pa by pumping using a turbomolecular pump (OSAKA VACUUM - TH520). A pulsed DC power supply (ENI, RPG-100) which can operate at pulse frequency of 150 kHz and at 2 kW was connected to the magnetron sputter target.

The sputtering was conducted at 0.67 Pa Ar and 300 W of time average power and, before deposition on the substrate, the sputter target was pre-sputtered for 5 min to clean the target surface and, during the deposition, the substrate maintained at room temperature was rotated at 15 rpm. As the sputter target, 3 in. diameter 99.99% pure Cu target (oxygen-free high-conductivity copper) was used and, as the substrate, 250 μm thick silicon wafers were used. Before the deposition, the silicon wafers were cleaned in sequence with acetone, icosapentaenoic acid, and deionized water in a ultrasonic cleaner for 15 min each. The thickness of Cu film deposited on the silicon wafer was maintained at ~10 μm.

The residual stress formed on the Cu film deposited silicon wafer was measured using a residual stress tester (JLCST022, J & L tech). This residual stress measurement device is measured by the method of the radius curvature stress. The laser specification used in this measurement is 1.0 mW of output power, 632.8 nm of wavelength, and 0.59 mm of beam diameter. Also, the lens shapes a plano-convex lens, and the laser spot was moved 25 mm for stress measuring from the center to the end on deposited film. Since the substrate is much thicker than the deposited Cu thin film, the residual stress σ of the film can be obtained using the following equation [19].

$$\sigma = \frac{1}{6R}\left[\frac{E_s}{(1-v_s)}\right]\left[\frac{s^2}{f}\right]$$

where $E_s$ is the Young's modulus of the substrate, $v_s$ is the Poisson's ratio of the substrate, and $1/R$ is the curvature of the substrate/deposited thin film composite, *s* is the thickness of substrate and *f* is the thickness of deposited thin film. This simple formula results from the following basic hypotheses: (a) strains and rotations are infinitesimal, (b) substrate and coating thicknesses are very small compared to the lateral dimensions of the plate and edges' effects are negligible, (c) coating thickness is small compared to substrate thickness ($f \ll s$), and (d) substrate and coating materials are homogeneous, isotropic, and linear elastic. The experimental error of the residual stress measurement was within ≤9.5%. And the morphology of the deposited Cu film was observed using a field emission SEM (S-4700, HITACHI) at 15 kV condition.

## 3. Results and discussion

### 3.1. Effect of pulse frequency

Cu film was deposited on silicon wafers as a function of pulse frequency (CW, 50 kHz, and 100 kHz) at 0.67 Pa Ar for 200 min while maintaining the time average power of 300 W. For the pulse frequency, the pulse duty ratio was kept at 80%. The residual stress and thickness of Cu film deposited on the silicon wafers as a function of pulse frequency are shown in Fig. 2. As shown in Fig. 2, due to the same time average power, the thickness of deposited Cu film was similar for different pulse frequency conditions including CW. However, as shown in Fig. 2, the increase of pulse frequency from CW to 100 kHz significantly decreased the residual stress of Cu from 21.75 MPa to 1.8 MPa.

To understand the reason for the decrease of residual stress of Cu film with increasing the pulse frequency, the characteristics of temporal voltage and current on the Cu target during the DC pulse magnetron sputtering were investigated and the results are shown in Fig. 3a and b, respectively, for the same conditions in Fig. 2. When the pulse frequency is varied from DC (0 Hz) to 100 kHz at the same time average power, total ion flux (that is, dose) to the Cu target is not significantly changed, and, as shown in Fig. 3b, the time average current is similar for DC, 50 kHz and 100 kHz indicating the total ion flux to the target is similar for different pulse frequency conditions. However, as shown in Fig. 3a and b, the peak voltage/peak current was varied from −330 V/0.91 A for DC to −670 V/3.2 A for 100 kHz, therefore, higher peak voltage/peak current was observed for the higher pulse frequency condition. The higher peak voltage with the higher peak current indicates higher instant Cu flux to the substrate for the higher pulse

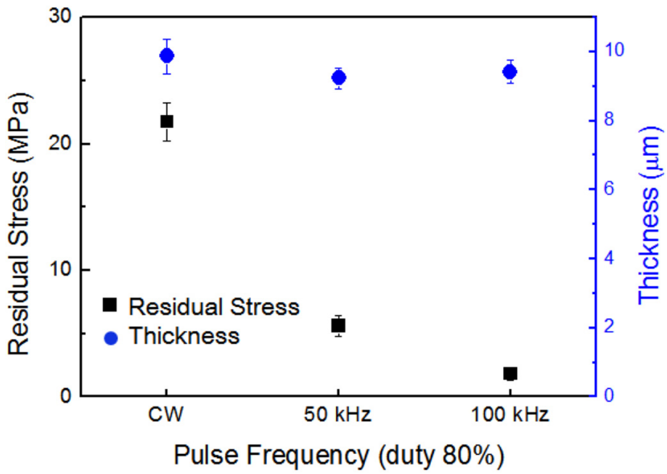


**Fig. 2.** Residual stress and the thickness of deposited Cu film as a function of pulse frequency (DC, 50 kHz, 100 kHz)while maintaining the average power of 300 W at 0.67 Pa Ar. The deposition time was 200 and the pulse duty ratio for 50 and 100 kHz was kept at 80%.

frequency condition. The higher sputtering voltage is also known to increase the energy of $Ar^+$ bombarding the substrate during the deposition [20,21].

The $Ar^+$ ion energy distribution on the substrate during the sputtering conditions in Fig. 2 was measured using the PSM located near the substrate location as a function of pulse frequency and the results are shown in Fig. 4. As shown, with the increasing the pulse frequency from CW to 100 kHz, the high energy tail was shifted toward higher ion energy indicating higher $Ar^+$ ion bombardment to the substrate for higher pulse frequency condition. The increased instant atom flux from the target and the higher $Ar^+$ ion bombardment energy during the deposition are known to form smaller grains on the substrate by increasing the nucleation rate on the substrate [22–25] and to increase the density of the deposited film by compacting effect [26], respectively.

### 3.2. Effect of pulse duty ratio

The effect of pulse duty ratio on the residual stress of Cu film deposited on the silicon substrate was investigated at 50 kHz pulse frequency and the results are shown in Fig. 5. The pulse duty ratio was varied from 60 to 90% while maintaining other conditions are the same as in Fig. 2. As shown in Fig. 5, due to the same average power of 300 W to the target during the sputtering, the thickness of Cu on the substrate was similar in the range of 9.18–9.74 µm after the deposition of

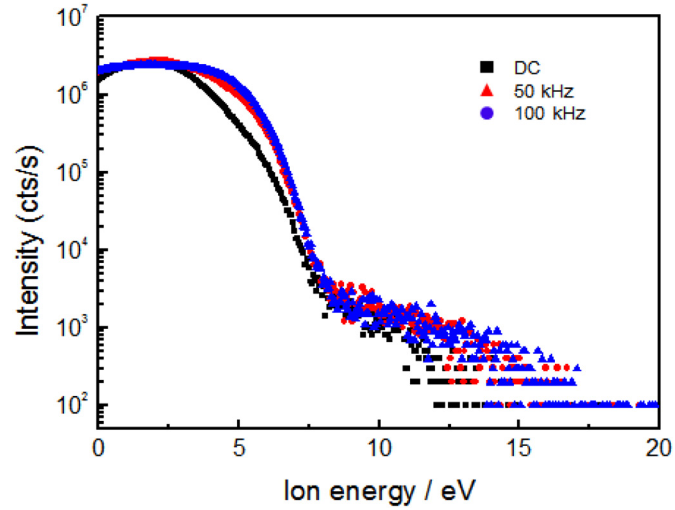


**Fig. 4.** $Ar^+$ ion energy distribution on the substrate measured for different pulse frequency (CW, 50 kHz, 100 kHz) of the DC pulse power in Fig. 2.

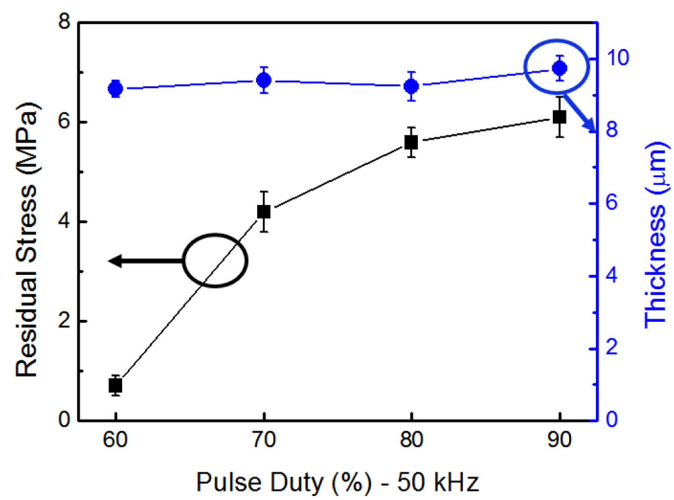


**Fig. 5.** Residual stress and the thickness of deposited Cu film as a function of pulse duty ratio (90%, 80%, 70%, 60%) while maintaining the average power of 300 W at 0.67 Pa Ar. The deposition time was 200 min and the pulse frequency was 50 kHz.

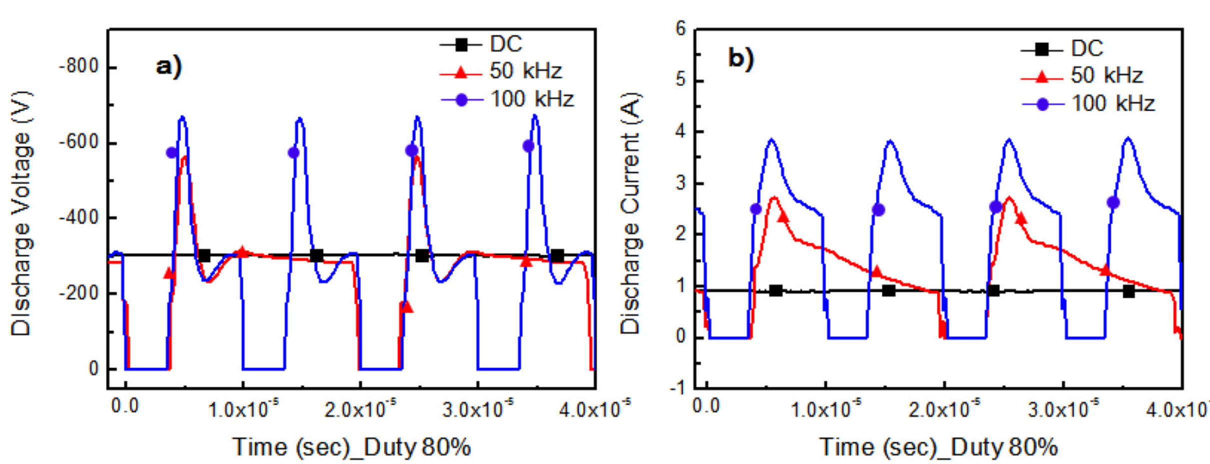


**Fig. 3.** Characteristics of (a) voltage and (b) current on the Cu target during the DC pulse sputtering as a function of pulse frequency (CW, 50 kHz, 100 kHz).in Fig. 2.

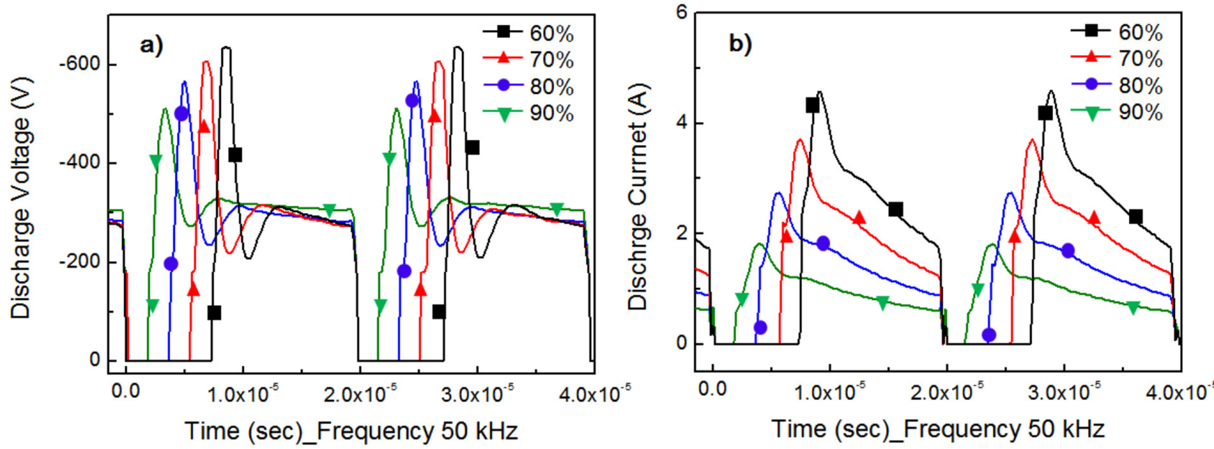


**Fig. 6.** Characteristics of (a) voltage and (b) current on the Cu target during the DC pulse sputtering as a function of pulse duty ratio (90%, 80%, 70%, 60%) in Fig. 5.

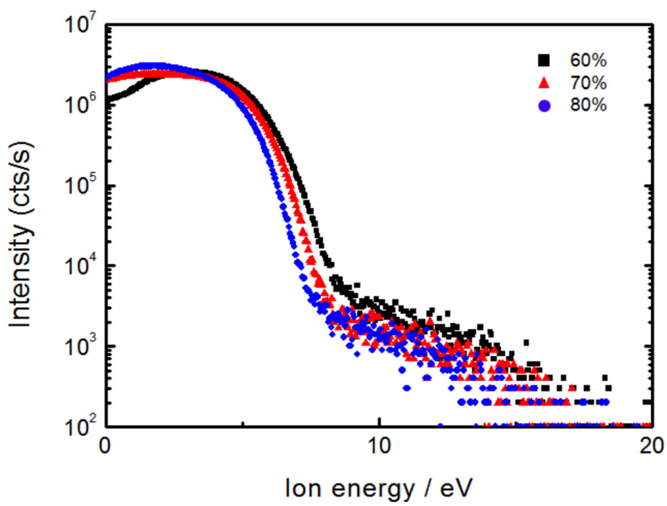


**Fig. 7.** $Ar^+$ ion energy distribution on the substrate measured for different pulse duty ratio (90%, 80%, 70%, 60%) of the DC pulse power in Fig. 5.

200 min. However, the decrease of pulse duty ratio at the time same average power from 90 to 60% decreased the residual stress of the Cu film from 6.1 MPa to 0.7 MPa.

The characteristics of temporal voltage and current on the Cu target during the DC pulse magnetron sputtering were also investigated as a function of duty ratio at 50 kHz of pulse frequency and at 300 W of time average power and the results are shown in Fig. 5a and b, respectively. As shown in Fig. 5, the lower duty ratio at the same power exhibited the higher peak voltage as well as higher peak current by varying from −510 V and 1.5 A at 90% to −635 V and 3.8 A at 60% with decreasing the duty ratio. Therefore, during each cycle of pulsing, higher instant Cu flux to the substrate is obtained at the lower duty ratio.

The energy of $Ar^+$ ion bombarding the substrate was also measured as a function of pulse duty ratio for the conditions in Fig. 5 and the results are shown in Fig. 6. As shown in Fig. 6, the lower pulse duty ratio exhibited the higher $Ar^+$ ion energy tail on the substrate surface indicating higher ion bombardment energy to the substrate at the lower pulse duty ratio when the pulse frequency is kept same (Fig. 7).

### 3.3. Effect on Cu film growth

Fig. 8a, b, and c show the Cu film morphology observed using a field emission SEM for different pulse frequency of DC, 50 kHz, and 100 kHz, respectively, for the condition shown in Fig. 2. As shown in Fig. 8, even though the decrease of grain size is not linearly proportional to the pulse frequency, the increase of pulse frequency decreased the grain size of Cu film deposited on the silicon substrate. The decrease of Cu grain size deposited on the substrate with increasing the pulse frequency at the same time average power is believed to be related to the instant high flux of Cu atoms by the instantly increased peak power voltage and current as shown in Fig. 3. The increased $Ar^+$ ion bombardment on the substrate with increasing the pulse frequency also appears to increase the Cu film density deposited on the substrate.

Fig. 9a, b, and c show the Cu film morphology for different pulse duty ratio of 80, 70, and 60%, respectively, for the condition shown in Fig. 5. As shown in Fig. 9, the grain size was decreased with decreasing the pulse duty ratio and the decrease of grain size was also related to the instant high Cu flux to the substrate during the pulsing by increasing the nucleation rate. Also, it is believed that the increased $Ar^+$ ion bombardment on the substrate with decreasing the pulse duty ratio increased the Cu film density deposited on the substrate.

It is investigated that the smaller grain size tends to exhibit lower residual stress of the film due to smaller differences in the growing grains in the film [27,28]. Also, the high flux and the high ion energy generated by pulsed power are expected to suppress tensile stress and lead to compressive stress in the film. These causes may also have

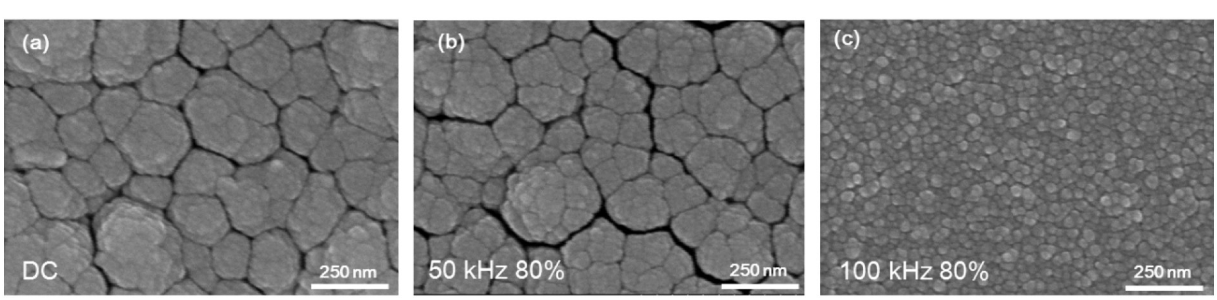


**Fig. 8.** Cu film surface images observed using a field emission SEM for different pulse frequency of (a) DC, (b) 50 kHz, and (c) 100 kHz shown in Fig. 2.

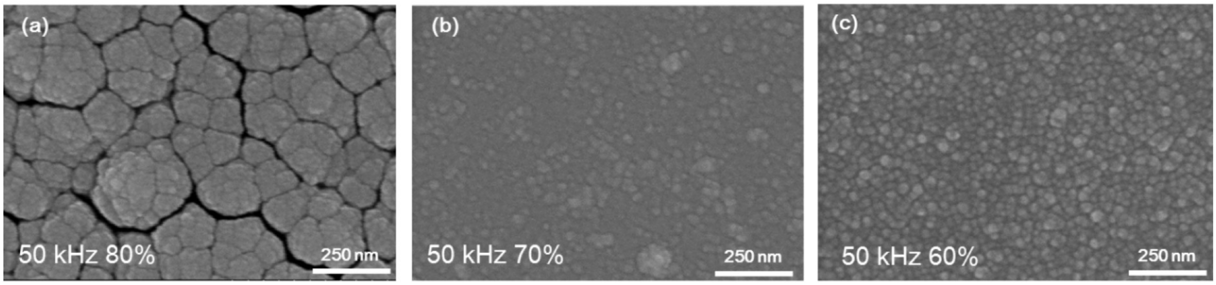


**Fig. 9.** Cu film surface images observed using a field emission SEM for different pulse duty ratio of 80, 70, and 60% shown in Fig. 2.

affected pulsed plasma lowering stress [29]. Therefore, it is believed that the lower residual stress obtained by the higher pulse frequency and lower pulse duty ratio in Figs. 2 and 5, respectively, is related to the smaller grain size of Cu film and the increased film density by the higher $Ar^+$ ion bombardment. In some cases, however, research has also been reported on the tendency of stress to decrease as the grain size increases. They reported that diffusion of atoms into grain boundaries and grain boundary densification are reasons for this phenomenon [29,30].

## 4. Conclusion

10 μm thick Cu film was deposited on the silicon substrate by DC pulse magnetron sputtering, and the effect of pulse frequency and pulse duty ratio on the residual stress of the deposited Cu film was investigated. The higher pulse frequency and the lower pulse duty ratio of the pulse power at the same average power decreased the residual stress of the deposited Cu film. It is believed that the lower residual stress of the deposited Cu film is related to the smaller grain size and higher film density of the deposited Cu film caused by the increased nucleation and increased $Ar^+$ ion bombardment on the substrate, respectively. The increased Cu nucleation at the higher pulse frequency and lower pulse duty ratio is believed to be from higher Cu atom flux to the substrate by instant higher voltage and higher current of sputtering power. By depositing Cu film with the pulse power composed of 50 kHz of pulse frequency and 60% pulse duty ratio, the significantly lower Cu residual stress of 0.7 MPa compared to 21.7 MPa of the Cu film deposited with DC power could be obtained. It is believed that, by using the higher pulse frequency with the lower pulse duty ratio, the further decreased residual film stress film can be obtained not only for Cu film but also for other metal films.

## Acknowledgments

This research was supported by the MOTIE (Ministry of Trade, Industry & Energy (10067827)) and Development of core-technology and components in organic electronics for ICT convergence support program for the development of the future display device.

## References

[1] H.H. Cheng, D.-S. Huang, M.-T. Lin, Heat dissipation design and analysis of high power LED array using the finite element method, Microelectron. Reliab. 52 (2012) 905.
[2] M.-S. Wu, K.H. Liu, Y.-Y. Wang, C.-C. Wan, Heat dissipation design for lithium-ion batteries, J. Power Sources 109 (2002) 160.
[3] H.-H. Wu, K.-H. Lin, S.-T. Lin, A study on the heat dissipation of high power multi-chip COB LEDs, Microelectron. J. 43 (2012) 280.
[4] D. Tuckerman, R. Pease, High-performance heat sinking for VLSI, IEEE Electron Device Lett. 2 (1981) 126.
[5] Y. Peles, A. Kosar, C. Mishra, C.-J. Kuo, B. Schneider, Forced convective heat transfer across a pin fin micro heat sink, Int. J. Heat Mass Transf. 48 (2005) 3615.
[6] M.J. Biercuk, M.C. Llaguno, M. Radosavljevic, J.K. Hyun, A.T. Johnson, J.E. Fischer, Carbon nanotube composites for thermal management, Appl. Phys. Lett. 80 (2002) 2767.
[7] Y. Wu, C.H. Liu, H. Huang, S.S. Fan, Effects of surface metal layer on the thermal contact resistance of carbon nanotube arrays, Appl. Phys. Lett. 87 (2005) 213108.
[8] J. Hone, M.C. Llaguno, M.J. Biercuk, A.T. Johnson, B. Batlogg, Z. Benes, J.E. Fischer, Thermal properties of carbon nanotubes and nanotube-based materials, Appl. Phys. A Mater. Sci. Process. 74 (2002) 339.
[9] M. Zhimin, R. Morjan, J. Anderson, E.E.B. Campbell, J. Liu, Proceedings of the IEEE 55th Electronic Components and Technology Conference, Lake Buena Vista, FL, 31 May, (2005), p. 51.
[10] M. Zhimin, J. Anderson, J. Liu, Proceedings of the IEEE 6th High Density Microsystem Design and Packaging and Component Failure Analysis Conference, Shanghai, China, 30 June, (2004), p. 373.
[11] K. Kordás, G. Tóth, P. Moilanen, M. Kumpumäki, J. Vähäkangas, A. Uusimäki, R. Vajtaia, P.M. Ajayan, Chip cooling with integrated carbon nanotube microfin architectures, Appl. Phys. Lett. 90 (2007) 123105.
[12] J.T. Gudmundsson, J. Alami, U. Helmersson, Evolution of the electron energy distribution and plasma parameters in a pulsed magnetron discharge, Appl. Phys. Lett. 78 (2001) 3427.
[13] V. Kouznetzov, K. Maca'k, J.M. Schnider, U. Helmersson, I. Petrov, A novel pulsed magnetron sputter technique utilizing very high target power densities, Surf. Coat. Technol. 122 (1999) 290.
[14] K.A. Aissa, A. Achour, J. Camus, L. Le Brizoual, P.-Y. Jouan, M.-A. Djouadi, Comparison of the structural properties and residual stress of AlN films deposited by dc magnetron sputtering and high power impulse magnetron sputtering at different working pressures, Thin Solid Films 550 (2014) 264.
[15] A.P. Ehiasarian, P.E. Hovsepian, L. Hultman, U. Helmersson, Comparison of microstructure and mechanical properties of chromium nitride-based coatings deposited by high power impulse magnetron sputtering and by the combined steered cathodic arc/unbalanced magnetron technique, Thin Solid Films 457 (2004) 270.
[16] A.P. Ehiasarian, W.-D. Münz, L. Hultman, U. Helmersson, I. Petrov, High power pulsed magnetron sputtered CrNx films, Surf. Coat. Technol. 163 (2003) 267.
[17] G. Greczynski, J. Lu, M.P. Johansson, J. Jensen, I. Petrov, J.E. Greene, L. Hultman, Role of Ti n+ and Al n+ ion irradiation (n = 1, 2) during $Ti_{1-x}Al_xN$ alloy film growth in a hybrid HIPIMS/magnetron mode, Surf. Coat. Technol. 206 (2012) 4202.
[18] Q. Luo, S. Yang, K.E. Cooke, Hybrid HIPIMS and DC magnetron sputtering deposition of TiN coatings: deposition rate, structure and tribological properties, Surf. Coat. Technol. 236 (2013) 13.
[19] L.B. Freund, Substrate curvature due to thin film mismatch strain in the nonlinear deformation range, J. Mech. Phys. Solids 48 (2000) 1159.
[20] N. Laegreid, G.K. Wehner, Sputtering yields of metals for Ar+ and ne+ ions with energies from 50 to 600 eV, J. Appl. Phys. 32 (1961) 365.
[21] D. Rosenberg, G.K. Wehner, Sputtering yields for low energy $He^+$-, $Kr^+$-, and $Xe^+$-ion bombardment, J. Appl. Phys. 33 (1962) 1842.
[22] D. Xu, V. Sriram, V. Ozolins, J.-M. Yang, K.N. Tu, G.R. Stafford, Carlos, In situ measurements of stress evolution for nanotwin formation during pulse electrodeposition of copper, J. Appl. Phys. 105 (2009) 023521.
[23] Y.M. Kim, M.J. Jung, S.G. Oh, J.G. Han, Spatially resolved optical emission spectroscopy of pulse magnetron sputtering discharge, Thin Solid Films 475 (2005) 91.
[24] Jeon G. Han, Recent progress in thin film processing by magnetron sputtering with plasma diagnostics, J. Phys. D. Appl. Phys. 42 (2009) 043001.
[25] Y.R. Park, D. Jung, K.-C. Kim, S.J. Suh, T.S. Park, Y.S. Kim, Physical properties of transparent conducting indium doped zinc oxide thin films deposited by pulsed DC magnetron sputtering, J. Electroceram. 23 (2009) 536.
[26] J. Lin, J.J. Moore, W.D. Sproul, B. Mishra, Z. Wu, J. Wang, The structure and properties of chromium nitride coatings deposited using dc, pulsed dc and modulated pulse power magnetron sputtering, Surf. Coat. Technol. 204 (2010) 2230.
[27] M.R. Barnett, Z. Keshavarz, A.G. Beer, D. Atwell, Influence of grain size on the compressive deformation of wrought Mg–3Al–1Zn, Acta Mater. 52 (2004) 5093.
[28] L. Cao, A. Sengupta, D. Pantuso, M. Koslowski, Effect of texture and grain size on the residual stress of nanocrystalline thin films, Model. Simul. Mater. Sci. Eng. 25 (2017) 075004.
[29] D. Magnfält, G. Abadias, K. Sarakinos, Atom insertion into grain boundaries and stress generation in physically vapor deposited films, Appl. Phys. Lett. 103 (2013) 051910.
[30] E. Chason, M. Karlson, J. Colin, D. Magnfalt, K. Sarakinos, G. Abadias, A kinetic model for stress generation in thin films grown from energetic vapor fluxes, J. Appl. Phys. 119 (2016) 145307.